Article

Not peer-reviewed version

Thermo-Mechanical Uniaxial Compression of 4D Printed PLA in Wide Range of Strain Rates and Temperatures below Glass Transition Temperature T_g

Vukašin Slavković *, Blaž Hanželič, Vasja Plesec, Strahinja Milenković, Gregor Harih

Posted Date: 6 May 2024

doi: 10.20944/preprints202405.0290.v1

Keywords: smart materials; shape memory polymer; 4D printing; thermo-mechanical cycle

Article

Thermo-Mechanical Uniaxial Compression of 4D Printed PLA in Wide Range of Strain Rates and Temperatures below Glass Transition Temperature T_g

Vukašin Slavković [1,*], Blaž Hanželič [2], Vasja Plesec [2], Strahinja Milenković [1] and Gregor Harih [2]

[1] Faculty of Engineering, University of Kragujevac, Sestre Janjic 6, 34000 Kragujevac, Serbia
[2] Laboratory for Integrated Product Development and CAD, Faculty of Mechanical Engineering, University of Maribor, Smetanova ulica 17, SI-2000 Maribor, Slovenia
* Correspondence: vukasin@fink.rs

Abstract: In this paper thermo-mechanical behavior of 4D printed Polylactic Acid (PLA) was investigated, focusing on its response to varying strain rates and temperatures below the glass transition temperature. Dynamic mechanical analysis and uniaxial tensile tests confirmed PLA's dependency on strain rate, showcasing its sensitivity to external stimuli. Stress-strain curves exhibited typical thermoplastic behavior, with yield stresses varying with strain rates, underscoring PLA's responsiveness to different deformation speeds. Clear strain rate dependence was observed, particularly at quasi-static rates, with temperature and strain rate fluctuations significantly influencing PLA's mechanical properties, including yield stress and deformation behavior. Isothermal compression tests demonstrated predictable stress-strain curves with distinct yield points, while adiabatic tests reveal additional complexities such as heat accumulation leading to further softening. Thermal imaging revealed temperature increase during deformation, highlighting the material's thermo-sensitive nature. These findings provide the basis for future research with the focus on advanced modeling techniques and mitigation strategies for self-heating effects, aiming to enhance PLA-based product reliability and performance in applications with deformations at higher strain rates, while also developing models to simulate shape recovery in 4D printed PLA structures at both cold and hot programming temperatures.

Keywords: smart materials; shape memory polymer; 4D printing; thermo-mechanical cycle

1. Introduction

Smart materials are prominent class of materials that have revolutionized both research and engineering. In general, materials with shape memory, usually named shape memory materials (SMM), are characterized by the shape memory effect (SME). SMMs are divided into several groups: Shape Memory Polymers (SMP), Shape Memory Alloys (SMA), Shape Memory Hydrogels (SMH) and Shape Memory Ceramics (SMC).SMPs can respond to a various external stimulus, and recover their deformed shape and return to their permanent shape from a programmed (temporary) shape under the influence of light [1,2], heat [3], magnetic [4], electricity [5], moisture [6], water [7,8]. SMAs for long have been the most prevalent, especially in human medicine [9], aerospace [10] and robotics [11]. Yet today, SMP and SMH are slowly taking the lead among other SMMs due to their broad applicability and relatively low cost of the raw material and manufacturing. The advantages of SMP and SMH over, primarily SMA, are that the stiffness can be adjusted in a wide glass transition temperature range T_g (55-100 °C) [12]. Besides that, SMPs are characterized by low density (≈1.2 g/cm^3), large deformations, biodegradability, biocompatibility, as well as low thermal conductivity

 doi:10.20944/preprints202405.0290.v1

[13,14]. SMPs can also restore shape after exposing to very large plastic deformations ≈500 %, while at SMA it is ≈6-7 %. In addition to mechanical, technological factors such as cost, fabrication, toxicity or recycling potential significantly affect the predominance of SMPs over SMAs [15] in the era of green technologies and green polymers [16].

The emergence of 4D printing represents an innovative fusion of smart materials and additive manufacturing techniques, propelling scientific exploration into material responsiveness to external stimuli and the development of intelligent structures for various applications. Smart materials in 4D printing adapt their properties or shapes in response to external stimuli. These materials can also harness energy, typically thermal, to perform mechanical tasks [17]. 4D printing technologies have facilitated scientific exploration into material research, stimulus responsiveness, mathematical modeling, and the subsequent development of intelligent structures. 4D printing has garnered increased interest lately, notably through the pioneering work of Professor Tibbits' research group at the Massachusetts Institute of Technology (MIT) [18]. Like most rapidly growing technologies, 4D printing relies on the rapid development of smart materials, 3D printers, mathematical modeling and design [19]. The Figure 1 shows that in contrast to 3D printing, the output product of 4D printing is an active or dynamic structure, which can be activated with appropriate external stimulus or energy input. The development of the new 4D printing industry is directly dependent on Material Science and the development of new materials. Besides materials growing and advancing in technologies such as Fused Deposition Modeling (FDM) [20] or Fused Filament Fabrication (FFF), Digital Light Processing (DLP) [21], Stereolithography (SLA) [22], Selective Laser Melting (SLM) and Inkjet [23,24] it is also a condition for further progress in this field. Various materials such as PVC [25,26], PETG [27], photopolymers [28] are used in 4D printing even a blends [29] and multimaterials for 3D printed auxetic structures [30] are used in 4D printing. This variety of materials, printing technologies and even creating composites opens completely new perspectives and possibilities for the use of 4D printing in various fields.

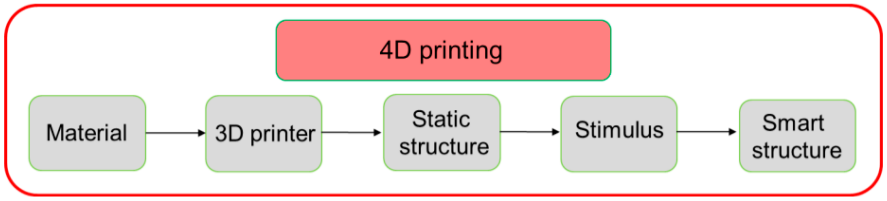

Figure 1. 4D printing concept with PLA material.

PLA is a material that has many applications, both in medicine and non-medical fields. One of its key features is its biocompatibility, which makes it safe to use in medical treatments. As it is a product of the human body and obtained from natural sources, it is also biodegradable. This is especially important for medical applications, where the device needs to be absorbed by the body after it has served its function.

There is a growing trend, of replacing devices made of metal or alloys with polymers to allow gradual healing of the diseased tissue through the mechanical weakening of the polymer devices. Additionally, as biodegradation occurs over time, there is no need for additional procedures to remove the device [31]. Due to the ability to customize the chemical structure and mechanical characteristics to the biochemical environment, PLA is widely used in biomedicine. It is used in various applications, including stents [32], orthopedic screws [33], supports for growing various cells, muscle tissue, bone and cartilage regeneration, planting osteogenic stem cells and implantation into bone defects [34] and drug delivery and delivery devices [35]. The use of PLA in additive manufacturing enables the production of complex biomedical devices based on computer-aided design and construction (CAD), in particular, with the use of patient-specific anatomical data, the creation of one-of-a-kind implants [36] and prosthesis socket [37]. A new challenge in the field of additive technologies is the application of 3D printing in the production of PLA composites, with or without reinforcement [38], scaffolds [39], biodegradable stents [40] and lately in auxtic energy

 doi:10.20944/preprints202405.0290.v1

absorption structures [41–47]. PLA can also be blended with other materials such as TPU in order to show that by changing the composition and programming temperature, the desired properties for different applications can be achieved so that the highest fixity, recovery, and stress recovery were obtained in hot, cold, and warm-programmed samples by manipulating the input energy and temperature [48]. Beside other thermoplastics used in FFF, PLA also shows potential for blending with natural materials such as wood [49].

In the last decade, the number of papers with mechanical tests of FFF samples has increased. In their paper [50], the authors compare the mechanical characteristics of the unidirectional, 3D-printed material with that of homogeneous injection-molded PLA, showing that manufacturing by 3D-printing and annealing improves toughness of samples. One of the latest research deals with the influence of strain rate and temperature on the mechanical behavior of PLA printed structure in tension [51]. Study aimed to analyze the effect of the infill line distance of 3D printed circular samples on their compressive elastic behavior during cyclic compressive loading [52]. In the paper presented in [53], uniaxial tensile responses of 3D-printed polylactic acid (PLA) samples following standard ASTM-D412 have been studied to characterize the mechanical properties at three temperatures: 30 °C, 40 °C, and 50 °C. Also, this study includes, quasi-static compressive experiments are performed on polymetric tubes with different temperatures. In this study [54] authors did experimental testing to determine compression performance and deformation behavior of 3D printed PLA lattice structures. In order to determine the influence of anisotropy and infill on the SME effect in printed materials, the authors in [55] examined the samples using uniaxial tensile tests and compressive tests are performed to study the effect of infill patterns on mechanical properties. Paper [56] presents experimental study of the compression uniaxial properties of PLA material manufactured with FFF in accordance with the requirements and conditions established in the ISO 604 standard characterizes the compression stiffness, the compression yield stress, the field of displacements, and stress along its elastic area until reaching the compression yield stress and the ultimate yield stress data showing that PLA material is promising for the manufacture of low volume industrial components that are subject to compression. Authors in [57] introduce a novel honeycomb structure that can enhance the compression property and energy absorption 4D printing with PLA materials showing that the novel honeycomb had a high compression property and had high energy absorption capacity. In this work [58], the influence of several factors such as printing temperature, bed temperature, printing speed, fan speed, and flow was studied showing that hat the parameters of extrusion-based 3D-printing influence the transformability of PLA-based materials. In this study [59], PLA is used in the 4D printing process for the manufacturing of complex geometry absorber components produced FFF varying printing parameters (temperature at the nozzle, the deposition speed, the layer thickness) and activation temperature. Experiments shown that components have good shape memory properties mostly influenced by activation temperature. Experimental tensile and compression tests are conducted in [60] on FFF PLA parts to evaluate the difference of main mechanical properties in tensile and compressive state. In this paper [61] monotonic, fatigue and creep behaviour of PLA under compression is studied, using cylindrical specimens tested according to ASTM D695 was conducted to identify and quantify the effects of printing parameters on the compression behavior of these specimens and failure mechanisms finding that compressive strength is linearly dependent with the density of the samples. In their paper [62] they examine PLA and PLA-Cu samples under both static and dynamic loading were studied using a universal testing machine and a split Hopkinson pressure bar apparatus showing that addition of copper powder increases the yield strength of the composite material significantly as compared to pure PLA, with both materials being strain rate sensitive. Also study [63] conducted the strain rate sensitivity of five thermoplastic materials (PLA, ABS, PC, CPE+ and nylon) under various tensile test speeds to study strain rate influence on mechanical characteristics of FFF 3D-printed materials. The influence of strain rate on tensile strength and yield strength in dynamic conditions is examined. Compression behavior of 4D printed metamaterials with various Poisson's ratios in [64] show the cellular metamaterials with zero Poisson's ratio possess superior vibration isolation capability compared to negative or positive Poisson's ratio cellular metamaterials at different deformation stages by a comprehensive analysis. A

 doi:10.20944/preprints202405.0290.v1

very detailed study presented in [65] describes the influence of printing parameters on the mechanical response of poly-lactic-acid (PLA), high-impact-polystyrene (HIPS), and acrylonitrile-butadiene-styrene (ABS) with special reference to shape memory in a 4D print while stretching at different speeds and at different temperatures. In order to examine the tensile strain rate performance of 3D printed PLA with various printing orientation in paper [66] conducted study using different deformation rates from the slowest to medium speed. The study, like most of the previous ones, shows different responses when the rate of deformation increases with an additional analysis of elongation and bending.

The aim of this paper is to extensively experimentally investigate the dependence of FFF printed PLA in a wide range of strain rates and temperatures in compression with large deformations. As due to high strain rates, test conditions can occur that are almost adiabatic, determining the existence of self heating in FFF PLA and the consequent additional softening, is a special challenge. All tests are carried out in coupled thermo-mechanical conditions so that the research results contribute to the expansion of knowledge in the field and provide new insight into the behavior of 4D printed PLA. There are several motivations for this study. The main motive is to determine all parameters related to macro mechanical characteristics of material, which will serve for the development of a coupled thermo-mechanical constitutive model for accurate modeling the behavior of the material using the Finite Element Method (FEM). Additionally, such an extensive study of coupled properties is not available to the authors' knowledge. The last and perhaps the most important motive is the possibility of expanding knowledge and further research in the field of auxetic structures, whose main mode of use and exploitation is radial and uniaxial compression at various strain rates. The study set up in this way could be the basis for successful and precise modeling of auxetics and metastructures in both cold and hot programming in consecutive research. The lower temperatures used in this research should serve to further focus on cold programming auxetics and research related to shape recovery by heating. Although the printing speeds and printing directions can also affect 4D printing properties, the focus of the study is on fully thermo-mechanically coupled characterization of PLA for the purposes of characterization and determination of characteristics for further development of the constitutive model.

In the Materials and Methods section, we present the rigorous materials and methods we used, such as filament used for 3D printing of samples, sample annealing procedure and uniaxial isothermal tensile filament and compression of cylindrical printed samples and DMTA. In the Results section we provide results obtained by uniaxial tensioning and uniaxial compression of samples obtained by 3D printing PLA as defined in previous section. Additionally, the results for DMTA analysis are provided. In Discussion section all results are discussed in the context of the paper main aims. We close in section Conclusion with most important findings and future suggestions.

2. Materials and Methods

2.1. Printing Samples

PLA samples were obtained by 3D printing from PLA filament with a diameter of 1.75 mm manufactured by Ultimaker. According to the manufacturer, the PLA material has a density of 1.24 $\frac{g}{cm^3}$, a melting rate during printing (MFR) of 6.09 $\frac{g}{10min}$ and a melting temperature of 145 - 160 ℃. Sample used in this study were made using FFF 3D printer UM2+ equipped with nozzle 0.4 mm, infill 100%, nozzle temperature 210 ℃, working plate temperature 60 ℃, layer deposition height of 0.1 mm and printing speed 40 $\frac{mm}{s}$. Cura (Ultimaker) slicer software was used for modelling, orientation and defining model supports. The model's orientation was selected to avoid the occurrence of barreling and buckling of the samples observed in previous studies, where it shown that these phenomena occur at a ration of height and diameter exceeding 2 [67–69] and according to standard for compression tests ASTM D695. All test were performed to obtain stress-strain curves at maximum safe strain value, e.g., before crack or fracture initiate in sample. It should be noted that although one of the main advantages of additive manufacturing is the printing speed, when considering smart materials in additive technologies, especially within 4D printing, the printing speed must be

 doi:10.20944/preprints202405.0290.v1

significantly reduced. As shown in [70] the production of samples in 4D printing at high printing speeds causes extremely high anisotropy due to residual thermal deformations. The parameters used in the production of PLA samples are shown in Table 1.

Table 1. Printing parameters of testing samples.

Parameter	Value
Nozzle diameter	0.4 mm
Layer height	0.1 mm
Infill	100 %
Printing speed	40 mm/s
Printing bed temperature	60 ℃
Production time	35 min

2.2. Dynamic Mechanical Thermal Analysis (DMTA) Measuring

Dynamic mechanical thermal analysis (DMTA) was conducted on a solid clamping tool for measurements according to DIN/ ISO 6721-1 with the use of Thermo Scientific™ HAAKE™ MARS™ Rheometers in combination with controlled test chamber (CTC). DMTA was performed in torsion with a rotational rheometer. The material hereby exposed to oscillatory shear while the temperature is changing continuously. Standard test prismatic PLA samples, dimensions 40x10x1 mm, were fabricated for DMTA, using same printing parameters that are given in Table 1. Geometry of DMTA test samples and 3D printing preview are shown in Figure 1. The experiment was performed in a temperature range of 40-80 °C, with strain amplitude 0.01 % and deformation frequency 1 Hz. The heating rate was set to 2 °C /min and samples were preheated from room temperature to 40 °C and then kept for 5 minutes at that temperature.

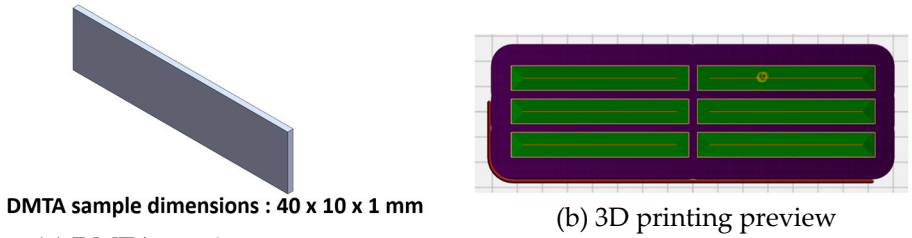

(a) DMTA specimen geometry (b) 3D printing preview

Figure 1. Geometrz of DMTA samples and 3D printing preview of slicing patterns.

2.3. Annealing Printed Specimen

After production, the samples were annealed in an oven at a temperature ≈20 °C higher than T_g and kept them at that temperature for a period of two hours. After that, the samples were slowly cooled in the oven, to room temperature, over a period of several hours. The procedure of annealing of samples after fabrication, provides a number of improvements including reducing of imperfections in the samples, reduced porositiy, better adhesion of material layers and improvement of the quality of surface layers. All samples used in the experiments were left in the oven environment (room temperature and humidity of 50%) in order to eliminate possible external influences and ageing of the material before testing.

2.4. Uniaxial tests

In order to determine the large deformation behaviour of 4D printed PLA polymer at various strain rates and temperatures lower then T_g , Shimadzu mun EHF-EV101K3-070-0A (Japan) universal testing machine equiped with with 100 kN calibrated load cell and thermal chamber is used. Displacement control during the test is performed via the Controller RS485, while the temperature in the temperature chamber is controlled via the EUROTHERM 2408 controller and the iTOOLS

 doi:10.20944/preprints202405.0290.v1

software package. As the diameter of the filament 1.75 mm is not adapted to the tension grips, the adaptive tool shown in Figure 3 is used during testing. Tensile tests were performed at room temperature for three strain rates 0.1, 0.01 and 0.001 s^{-1}.

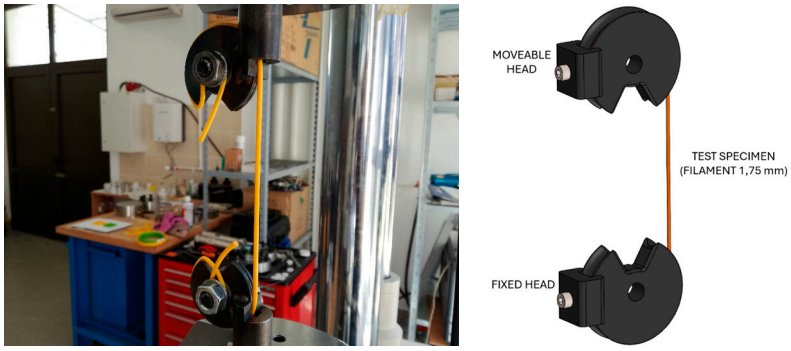

Figure 3. Uniaxial tensile testing of filament procedure (left) equipment for uniaxial filament testing and (right) sketch of equipment.

To measure the thermo-mechanical properties of the samples in uniaxial compression at various temperatures, Shimadzu mun EHF-EV101K3-070-0A universal testing machine equipped with 100 kN calibrated load cell and thermal chamber is used. Thermocouples were placed close to the surface and at the height of the sample as the temperature of the chamber in the sample zone was maintained. As already mentioned, cylindrical samples with a height and diameter of 10 mm were used, the ratio of height and diameter was chosen in order to avoid the occurrence of barreling and buckling of the samples observed in previous studies, where it is shown that these phenomena occur at a ratio of height and diameter exceeding 2. To reduce the friction Teflon strips were placed between the sample and the surface of the compression platens. The procedure of isothermal tests was defined as follows: the specimen was placed on a previously applied Teflon (PTFE) strip on the bottom compression platen, then the chamber was heated to the desired test temperature. In order to achieve temperature equilibrium, the specimen was kept in the heated chamber ≈30 minutes before starting the uniaxial compression test. For compression tests, the upper moving platen moves freely for given displacement at constant velocity. All successful experiments were repeated three times for each strain rate and temperature (36 specimen in total) to ensure repeatability of results and exclude potential mistakes. Uniaxial compression experiments were conducted at four different strain rates 0.1 s^{-1}, 0.01 s^{-1}, 0.001 s^{-1} and 0.0001 s^{-1} and three temperatures 25 °C, 37 °C and 50 °C.

2.5. Measurement of Temperature Change at High Strain Rates

The subject of the test is PLA, which, in addition to the shape memory effect during 4D printing, is also characterized by an increase in temperature during testing at high deformation rates. The measurement of temperature increase in the samples was performed at room temperature and deformation rates of 0.01 s^{-1} and 0.1 s^{-1}. Even before the initial tests, these strain rates were identified as those for which an almost adiabatic scenario is established for thermoplastics [71–74]. Flir I7 infrared camera was used for the measurement of temperature evolution during compression tests.

3. Results and Discussion

3.1. DMTA Results

Figure 4 and Table 2 show the results of measuring the transition temperature T_g and the change of the storage modulus G', loss modulus G'' and loss tangent tan del with temperature obtained by DMTA tests. The Figure allows identifying three characteristic zones of shape memory material: glass transition (blue surface in the picture), solid or glassy phase with high values of elastic modulus (left of the glass transition zone) and rubbery or soft phase of low values of elastic modulus (right of the transition zone). The results are in agreement with previous studies [75,76] for 4D printed PLA. The

 doi:10.20944/preprints202405.0290.v1

glass transition temperature of PLA whose position is defined by the peak of loss tangent (tan delta) is approximately at T_g = 65 °C, at which a significant drop in the elastic modulus occurs. The values for storage modulus in glassy phase are ≈1045.7 MPa and storage modulus in rubber phase ≈1.2 MPa and their high ratio (more than two orders of magnitude) show great shape memory potential of 4D printed PLA [77]. In general, these values show good shape fixity and good mechanical properties of material at lower temperatures and potential for large deformations at higher temperatures. Also, these values indicate that material is very sensitive to temperature which makes 4D printed PLA ideal candidate for further shape recovery research in auxetics.

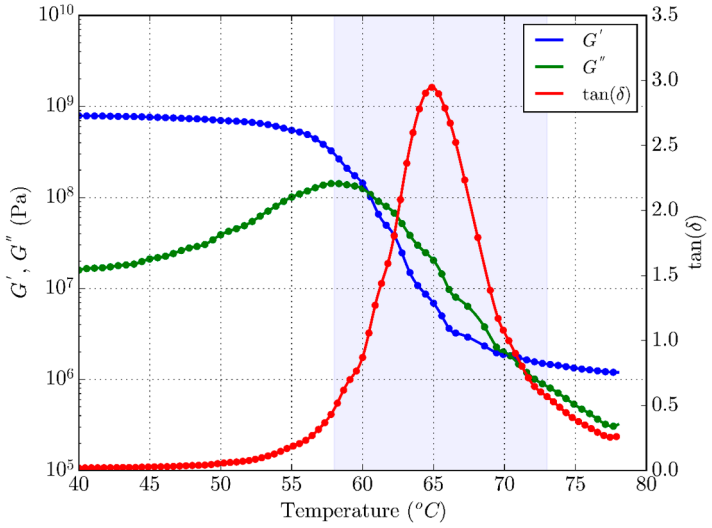

Figure 4. DMTA results for 4D printed PLA.

Table 2. DMTA results.

G′ (MPa)	G″ (MPa)	G′/G″ (-)	T_g (°C)
1045	1.2	>100	65

3.2. Uniaxial Tensile Tests of Filament

This section provides confirmation of the dependence of the base material PLA, used for printing the samples, on the deformation rate. As expected, Figure 5 shows a typical distribution of curves for thermoplastic materials that depend on the rate of deformation. At all three deformation rates, the elastic range up to the point of over-yielding is expressed. The non-linear increase in stress follows up to the yield point, which is also the point of the highest stress, after which deformational softening of the material follows. The yield stresses are 55 MPa, 48 MPa and 42 MPa for strain rates of 0.01 s^{-1}, 0.001 s^{-1} and 0.0001 s^{-1} respectively. Also, all yield points lie in range 6-8 % of deformation.

 doi:10.20944/preprints202405.0290.v1

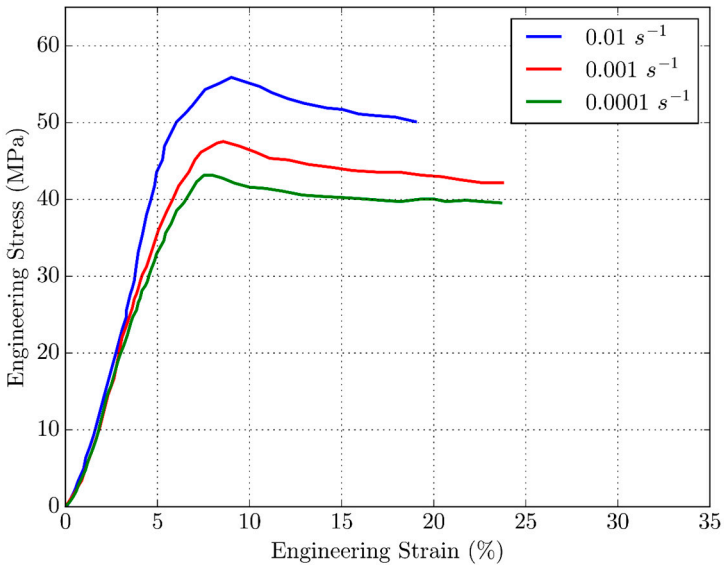

Figure 5. Stress-strain curves for PLA filament at various strain rates.

3.3. Uniaxial Compression Testing

We have conducted a series of uniaxial compression experiments on the 4D printed PLA. All tests were carried for temperatures below determined T_g=65 °C. The uniaxial compression experiments were carried at true-strain rates 0.0001 s^{-1}, 0.001 s^{-1}, 0.01 s^{-1} and 0.1 s^{-1} at 25 °C, 37 °C and 50 °C up to strain levels of ≈50 % (0.68 true strain). Since the drop of the mechanical response is observed for the strain rates 0.01 s^{-1} and 0.1 s^{-1} at large strains (>0.4 true strain) we separate analysis of results in two groups, isothermal at strain rates 0.0001 s^{-1} and 0.001 s^{-1} and adiabatic at strain rates 0.01 s-1 and 0.1 s^{-1}. Figure 6 shows as printed cylindrical samples and sample after compression to 0.5 of initial height.

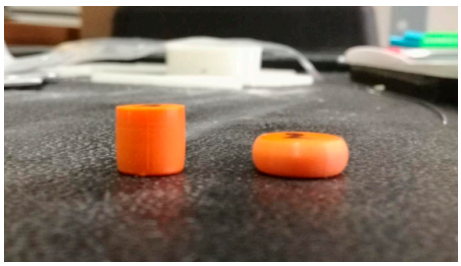

Figure 6. PLA 4D printed cylindrical samples – as printed (left) and after compression (right).

At isothermal experimental conditions 4D printed PLA polymer exhibits a strain-rate and temperature-dependent response typical for solid or glassy phase. True strain-stress isothermal uniaxial compression experimental results are given in Figure 2 and Figure 3. The material shows a tendency of glassy polymer behaviour under T_g with initial elastic region and rate dependent yield point, followed by strain softening. For higher values of strain, in case of both strain rates the curves are parallel and there is no intersection between them, so it can be concluded that there is no additional weakening of the samples during large deformations. The figure clearly shows the characteristics of the solid phase of PLA (temperatures below T_g) material response with clearly defined yield point, followed by strain softening, and strain hardening of the material at large deformations. With temperature rise from 25 °C to 50 °C yield stress decreases from ≈80 MPa to ≈40 MPa. Upon unloading about approximately 4 % strain is reversible with temperature held constant. Increasing the temperature at the same strain rate leads to a drop in the value of the yield stress, as well as the stress during deformation hardening but the amount of hardening at larger strains is

 doi:10.20944/preprints202405.0290.v1

slightly affected for this temperature range. A certain regularity can be observed in the stress distribution, except for minor measurement deviations for temperatures of 37 °C. Even for the very large strains there is no intersection of flow curves which indicates that no additional softening caused by strain rate occurred.

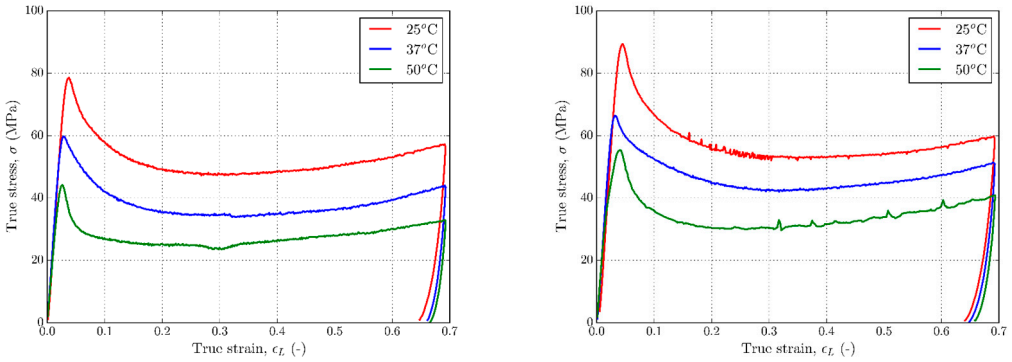

(a) 0.0001 s^{-1} (b) 0.001 s^{-1}

Figure 2. Stress – strain curves for PLA at strain rates (a) 0.0001 s^{-1} and (b) 0.001 s^{-1}.

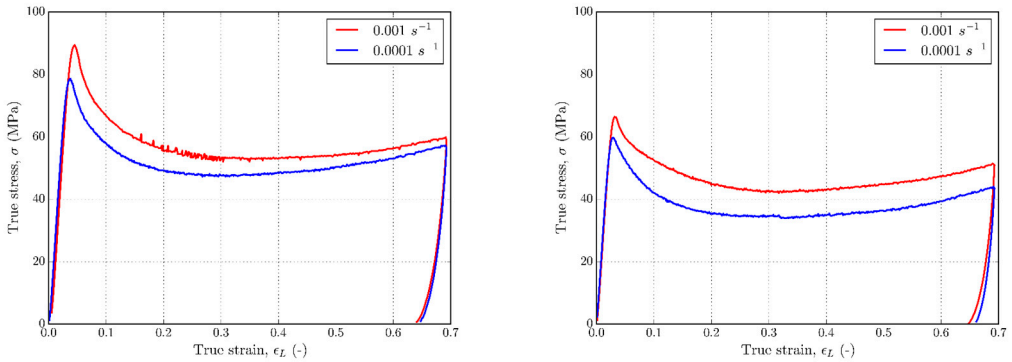

(a) 25 °C (b) 37 °C

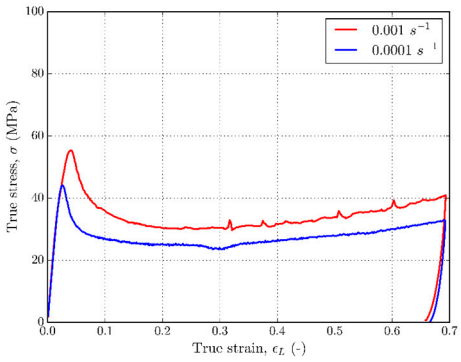

(c) 50 °C

Figure 3. Stress – strain curves for PLA at temperatures (a) 25 °C, (b) 37 °C and (c) 50 °C.

True strain-stress isothermal uniaxial compression experimental results are given if Figure 4 and Figure 5. The material shows a tendency of glassy polymer behaviour, initial elastic region with rate dependent yield stress point, followed by deformation softening. For higher values of strain, in case of both strain rates, heat could not be dissipated to the surrounding, which is clear explanation for crossing of curves at higher strains which is in correlation with tensile [78] and compression [72,73] results of previous studies. It should be noted that a 0.001 s^{-1} strain rate curve has been added to this diagram in order to show the amount of softening and make a clear distinction between isothermal and adiabatic strain rates. In this case material shows a tendency of glassy polymer behaviour under T_g with initial elastic region and rate dependent yield point, followed by strain softening. For higher

 doi:10.20944/preprints202405.0290.v1

values of strain, in case of both strain rates the curves are parallel and there is no intersection between them, so it can be concluded that there is no additional weakening of the samples during large deformations. The figure clearly shows the characteristics of the solid phase of PLA (temperatures below T_g) material response with clearly defined yield point, followed by strain softening, and strain hardening of the material at large deformations. With temperature rise from 25 °C to 50 °C yield stress decreases from ≈110 MPa to ≈50 MPa. Upon unloading about ≈5% strain is reversible with temperature held constant. Increasing the temperature at the same strain rate leads to a drop in the value of the yield stress, as well as the stress during deformation hardening but the amount of hardening at larger strains is slightly affected for this temperature range. A certain regularity can be observed in the stress distribution, except for minor measurement deviations for temperatures of 37 °C. Even for the very large strains there is no intersection of flow curves which indicates that no additional softening caused by strain rate occurred.

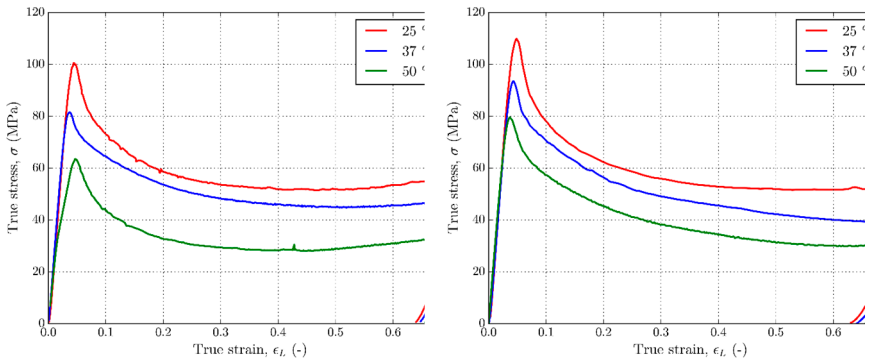

(a) 0.01 s^{-1} (b) 0.1 s^{-1}

Figure 4. Stress – strain curves for PLA at strain rates (a) 0.01 s^{-1} and (b) 0.1 s^{-1}.

The analysis of the same strain-stress curves grouped according to the temperatures gives a slightly different picture of the phenomenon taking place in the material. Figure 5 shows flow curves for 25 °C, 37 °C, 50 °C and strain rates 0.1 s^{-1}, 0.01 s^{-1} and 0.001 s^{-1}. The characteristics that can be observed on the stress-strain curves are yield curves have a clearly defined yield point like curves grouped by strain rate and after unloading ≈5% of strain is reversible. There is an intersection of the strain-stress curves, due to the stress drop at strain rates of 0.1 s^{-1} and 0.01 s^{-1}, at deformation ≈0.5 which is in agreement with the results for thermoplastics [74,79,80]. The stress drop is a consequence of the self heating in case of both strain rates, heat could not be dissipated to the surrounding because of speed of the process which consequently leads to further softening of thermo sensitive material.

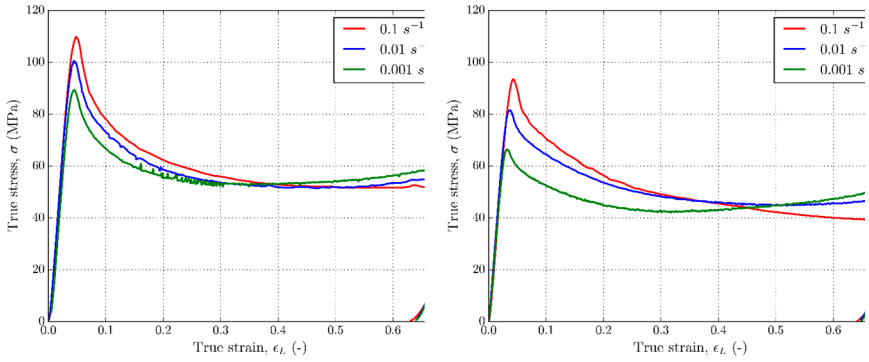

(a) 25 °C (b) 37 °C

Preprints.org (www.preprints.org) | NOT PEER-REVIEWED | Posted: 6 May 2024 doi:10.20944/preprints202405.0290.v1

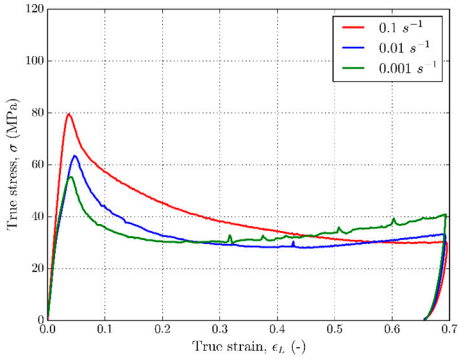

(c) 50 °C

Figure 5. Stress – strain curves for PLA at temperatures (a) 25 °C, (b) 37 °C and (c) 50 °C.

Values of yield stress dependence on strain rate and temperature are summarized in Figure 6.

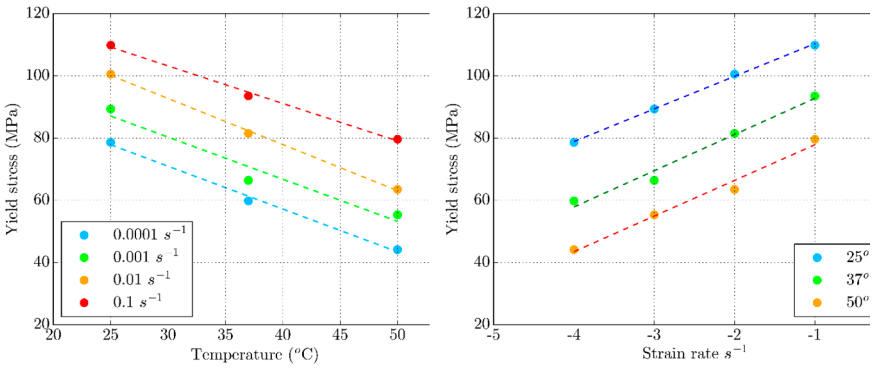

(a) temperature (b) strain rates

Figure 6. Yield stress values dependence on (a) temperature and (b) strain rate.

3.4. Adiabatic Tests with Self Heating and Strain Softening

In this section, we present the results of self-heating in the material at strain rates greater than 0.01 s^{-1} and that the mentioned processes can be considered almost adiabatic. A typical thermo-mechanical coupled curve is shown in Figure 11. The temperature was recorded with a thermal imaging camera in 5 points for the PLA sample at a deformation rate of 0.01 s^{-1}. The recording shows that the temperature on the surface of the sample increases monotonously, with the temperature rising from 25 °C (room temperature) to ≈ 40 °C . Although this temperature is below the determined Tg for PLA, as shown on the stress-strain curves, there is a drop in mechanical characteristics that can be attributed to the internal heating of the extremely thermo-sensitive material. Maximum temperature was consistently observed in the middle of the sample. It also shown that the increase in temperature is insignificant before the flow in mateiral and that the temperature continues to rise constantly. Immediately after the start of unloading a temperature drop of ≈ 2 °C is observed.

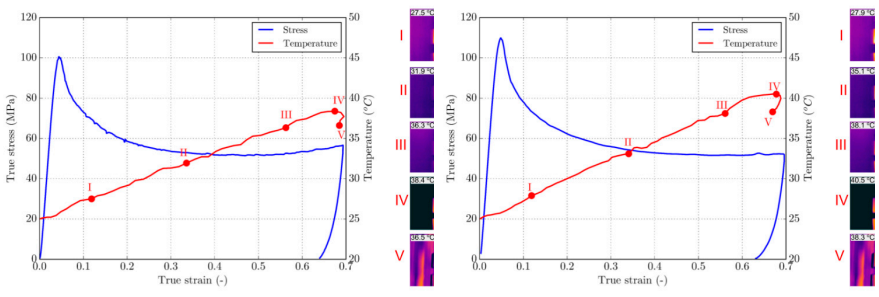

(a) 0.01 s^{-1} (b) 0.1 s^{-1}

Figure 12. Temperature evolution of 4D printed PLA at strain rate (a) 0.01 s^{-1} and (b) 0.1 s^{-1}.

 doi:10.20944/preprints202405.0290.v1

Future research should focus on advanced modeling techniques to predict material behavior and explore mitigation strategies for self-heating effects, enhancing PLA-based product reliability and performance in applications with deformations at higher strain rates. The observed adiabatic processes that take place in the material during deformation at high strain rates require the development of a FEM coupled thermo-mechanical constitutive model in order to simulate self-heating processes with sufficient accuracy. In addition, the ultimate goal of the following research is to expand the FEM model with the ability to simulate shape recovery in 4D printed PLA samples and structures, both at cold (temperatures below T_g) and hot programming (temperatures over T_g). The aspect of cold programming is particularly important, because most auxetic structures and metamaterials undergo deformation at temperatures lower than T_g, and the simulation of shape recovery occurs by heating above T_g.

4. Conclusions

The study confirmed PLA material's dependency on strain rate, with stress-strain curves displaying typical thermoplastic behavior. Yield stresses varied with strain rates, underscoring the material's sensitivity to deformation rates. Samples exhibited clear strain rate dependence, particularly at quasi-static rates, with temperature and strain rate variations significantly impacting mechanical properties, including yield stress and deformation behavior. Isothermal compression tests showed predictable stress-strain curves with distinct yield points, while adiabatic tests revealed additional complexities such as heat accumulation leading to further softening. Observations at higher strain rates indicated self-heating phenomena in PLA, resembling adiabatic conditions. Thermal imaging revealed temperature increases during deformation, with maximum temperatures at the sample center. The drop in mechanical characteristics attributed to internal heating highlighted the material's thermo-sensitive nature. These findings deepen the understanding of PLA behavior and hold significant implications for practical applications, especially in 3D and 4D printing and manufacturing.

Author Contributions: Conceptualization, V.S. and G.H.; methodology, V.S., B.H. and G.H..; software, V.S. and B.H.; validation, V.S., B.H. and S.M.; formal analysis, V.S. and G.H.; investigation, V.S., B.H. and G.H.; resources, V.S.; data curation, V.S., V.P. and B.H.; writing—original draft preparation, V.S., G.H., B.H, V.P. and S.M.; writing—review and editing, V.S., G.H., B.H, V.P. and S.M.; visualization, V.S., B.H. and S.M.; supervision, G.H.; funding acquisition, G.H. All authors have read and agreed to the published version of the manuscript.

Funding: The authors acknowledge the financial support from the Slovenian Research Agency (Research Core Funding No. P2-0063.

Institutional Review Board Statement: Not applicable.

Data Availability Statement: Not applicable.

Acknowledgments: Not applicable.

Conflicts of Interest: The authors declare no conflicts of interest.

References

1. Lendlein, A.; Jiang, H.; Jünger, O.; Langer, R. Light-Induced Shape-Memory Polymers. *Nature* **2005**, *434*, 879–882, doi:10.1038/nature03496.
2. Lee, K.M.; Koerner, H.; Vaia, R.A.; Bunning, T.J.; White, T.J. Light-Activated Shape Memory of Glassy, Azobenzene Liquid Crystalline Polymer Networks. *Soft Matter* **2011**, *7*, 4318–4324, doi:10.1039/C1SM00004G.
3. Heuchel, M.; Sauter, T.; Kratz, K.; Lendlein, A. Thermally Induced Shape-Memory Effects in Polymers: Quantification and Related Modeling Approaches. *Journal of Polymer Science Part B: Polymer Physics* **2013**, *51*, 621–637, doi:https://doi.org/10.1002/polb.23251.
4. Razzaq, M.Y.; Behl, M.; Nöchel, U.; Lendlein, A. Magnetically Controlled Shape-Memory Effects of Hybrid Nanocomposites from Oligo(Omega-Pentadecalactone) and Covalently Integrated Magnetite Nanoparticles. *Polymer* **2014**, *55*, 5953–5960, doi:https://doi.org/10.1016/j.polymer.2014.07.025.

5. Schmidt, A.M. Electromagnetic Activation of Shape Memory Polymer Networks Containing Magnetic Nanoparticles. *Macromolecular Rapid Communications* **2006**, *27*, 1168–1172, doi:https://doi.org/10.1002/marc.200600225.
6. Garces, I.T.; Aslanzadeh, S.; Boluk, Y.; Ayranci, C. Effect of Moisture on Shape Memory Polyurethane Polymers for Extrusion-Based Additive Manufacturing. *Materials (Basel, Switzerland)* **2019**, *12*, 244, doi:10.3390/ma12020244.
7. Liu, Y.; Li, Y.; Chen, H.; Yang, G.; Zheng, X.; Zhou, S. Water-Induced Shape-Memory Poly(D,L-Lactide)/Microcrystalline Cellulose Composites. *Carbohydrate polymers* **2014**, *104*, 101—108, doi:10.1016/j.carbpol.2014.01.031.
8. Bai, Y.; Chen, X. A Fast Water-Induced Shape Memory Polymer Based on Hydroxyethyl Cellulose/Graphene Oxide Composites. *Composites Part A: Applied Science and Manufacturing* **2017**, *103*, 9–16, doi:https://doi.org/10.1016/j.compositesa.2017.09.003.
9. Petrini, L.; Migliavacca, F. Biomedical Applications of Shape Memory Alloys. *Journal of Metallurgy* **2011**, *2011*, 501483, doi:10.1155/2011/501483.
10. Hartl, D.J.; Lagoudas, D.C. Aerospace Applications of Shape Memory Alloys. *Proceedings of the Institution of Mechanical Engineers, Part G: Journal of Aerospace Engineering* **2007**, *221*, 535–552, doi:10.1243/09544100JAERO211.
11. Kheirikhah, M.M.; Rabiee, S.; Edalat, M.E. A Review of Shape Memory Alloy Actuators in Robotics. In Proceedings of the RoboCup 2010: Robot Soccer World Cup XIV; Ruiz-del-Solar, J., Chown, E., Plöger, P.G., Eds.; Springer Berlin Heidelberg: Berlin, Heidelberg, 2011; pp. 206–217.
12. Erkeçoğlu, S.; Sezer, A.D.; Bucak, S. Smart Delivery Systems with Shape Memory and Self-Folding Polymers. In *Smart Drug Delivery System*; Sezer, A.D., Ed.; IntechOpen: Rijeka, 2016.
13. Korde, J.M.; Kandasubramanian, B. Naturally Biomimicked Smart Shape Memory Hydrogels for Biomedical Functions. *Chemical Engineering Journal* **2020**, *379*, 122430, doi:https://doi.org/10.1016/j.cej.2019.122430.
14. Huang, W.M.; Ding, Z.; Wang, C.C.; Wei, J.; Zhao, Y.; Purnawali, H. Shape Memory Materials. *Materials Today* **2010**, *13*, 54–61, doi:https://doi.org/10.1016/S1369-7021(10)70128-0.
15. Liu, C.; Qin, H.; Mather, P.T. Review of Progress in Shape-Memory Polymers. *J. Mater. Chem.* **2007**, *17*, 1543–1558, doi:10.1039/B615954K.
16. Hasan, M.R.; Davies, I.J.; Pramanik, A.; John, M.; Biswas, W.K. Potential of Recycled PLA in 3D Printing: A Review. *Sustainable Manufacturing and Service Economics* **2024**, *3*, 100020, doi:https://doi.org/10.1016/j.smse.2024.100020.
17. Mehrpouya, M.; Vahabi, H.; Janbaz, S.; Darafsheh, A.; Mazur, T.R.; Ramakrishna, S. 4D Printing of Shape Memory Polylactic Acid (PLA). *Polymer* **2021**, *230*, 124080, doi:https://doi.org/10.1016/j.polymer.2021.124080.
18. Tibbits, S. The Emergence of "4D Printing." *TED Conference* **2013**.
19. Liu, Y.; Zhang, W.; Zhang, F.; Lan, X.; Leng, J.; Liu, S.; Jia, X.; Cotton, C.; Sun, B.; Gu, B.; et al. Shape Memory Behavior and Recovery Force of 4D Printed Laminated Miura-Origami Structures Subjected to Compressive Loading. *Composites Part B: Engineering* **2018**, *153*, 233–242, doi:https://doi.org/10.1016/j.compositesb.2018.07.053.
20. Dudek, P. FDM 3D Printing Technology in Manufacturing Composite Elements. *Archives of Metallurgy and Materials* **2013**, *Vol. 58, iss. 4*, 1415–1418, doi:10.2478/amm-2013-0186.
21. Jasveer, S.; Jian-bin, X. Comparison of Different Types of 3 D Printing Technologies.; 2018.
22. Kuang, X.; Zhao, Z.; Chen, K.; Fang, D.; Kang, G.; Qi, H.J. High-Speed 3D Printing of High-Performance Thermosetting Polymers via Two-Stage Curing. *Macromolecular Rapid Communications* **2018**, *39*, 1700809, doi:https://doi.org/10.1002/marc.201700809.
23. Soleimani-Gorgani, A. 14 - Inkjet Printing. In *Printing on Polymers*; Izdebska, J., Thomas, S., Eds.; William Andrew Publishing, 2016; pp. 231–246 ISBN 978-0-323-37468-2.
24. Riheen, M.A.; Saha, T.K.; Sekhar, P.K. Inkjet Printing on PET Substrate. *Journal of The Electrochemical Society* **2019**, *166*, B3036–B3039, doi:10.1149/2.0091909jes.
25. Aberoumand, M.; Soltanmohammadi, K.; Rahmatabadi, D.; Soleyman, E.; Ghasemi, I.; Baniassadi, M.; Abrinia, K.; Bodaghi, M.; Baghani, M. 4D Printing of Polyvinyl Chloride (PVC): A Detailed Analysis of Microstructure, Programming, and Shape Memory Performance. *Macromolecular Materials and Engineering* **2023**, *308*, 2200677, doi:https://doi.org/10.1002/mame.202200677.
26. Aberoumand, M.; Rahmatabadi, D.; Soltanmohammadi, K.; Soleyman, E.; Ghasemi, I.; Baniassadi, M.; Abrinia, K.; Bodaghi, M.; Baghani, M. Stress Recovery and Stress Relaxation Behaviors of PVC 4D Printed by FDM Technology for High-Performance Actuation Applications. *Sensors and Actuators A: Physical* **2023**, *361*, 114572, doi:https://doi.org/10.1016/j.sna.2023.114572.

27. Soleyman, E.; Rahmatabadi, D.; Soltanmohammadi, K.; Aberoumand, M.; Ghasemi, I.; Abrinia, K.; Baniassadi, M.; Wang, K.; Baghani, M. Shape Memory Performance of PETG 4D Printed Parts under Compression in Cold, Warm, and Hot Programming. *Smart Materials and Structures* **2022**, *31*, 085002, doi:10.1088/1361-665X/ac77cb.
28. Sælen, R.L.; Hopperstad, O.S.; Clausen, A.H. Mechanical Behaviour and Constitutive Modelling of an Additively Manufactured Stereolithography Polymer. *Mechanics of Materials* **2023**, *185*, 104777, doi:https://doi.org/10.1016/j.mechmat.2023.104777.
29. Mirasadi, K.; Rahmatabadi, D.; Ghasemi, I.; Khodaei, M.; Baniassadi, M.; Baghani, M. Investigating the Effect of ABS on the Mechanical Properties, Morphology, Printability, and 4D Printing of PETG-ABS Blends. *Macromolecular Materials and Engineering n/a*, 2400038, doi:https://doi.org/10.1002/mame.202400038.
30. Mehrpouya, M.; Ghalayaniesfahani, A.; Postmes, J.F.; Gibson, I. Tailoring Mechanical Properties in 3D Printed Multimaterial Architected Structures. *Journal of the Mechanical Behavior of Biomedical Materials* **2024**, *152*, 106431, doi:https://doi.org/10.1016/j.jmbbm.2024.106431.
31. Hamad, K.; Kaseem, M.; Yang, H.W.; Deri, F.; Ko, Y.G. Properties and Medical Applications of Polylactic Acid: A Review. *eXPRESS Polymer Letters* **2015**, *9*, 435–455, doi:10.3144/expresspolymlett.2015.42.
32. Soares, J.S.; Moore, J.E.; Rajagopal, K.R. Constitutive Framework for Biodegradable Polymers with Applications to Biodegradable Stents. *ASAIO Journal* **2008**, *54*, 295–301.
33. Haers, P.E.; Suuronen, R.; Lindqvist, C.; Sailer, H. Biodegradable Polylactide Plates and Screws in Orthognathic Surgery: Technical Note. *Journal of Cranio-Maxillo-Facial Surgery* **2010**, *26*, 87–91, doi:https://doi.org/10.1016/S1010-5182(98)80045-0.
34. Wiebe, J.; Nef, H.M.; Hamm, C.W. Current Status of Bioresorbable Scaffolds in the Treatment of Coronary Artery Disease. *JOURNAL OF THE AMERICAN COLLEGE OF CARDIOLOGY* **2014**, *64*, 415–424, doi:doi.org/10.1016/j.jacc.2014.09.041.
35. Lasprilla, A.J.R.; Martinez, G.A.R.; Lunelli, B.H.; Jardini, A.L.; Filho, R.M. Poly Lactic Acid Synthesis for Application in Biomedical Devices — A Review. *Biotechnology Advances* **2012**, *30*, 321–328, doi:https://doi.org/10.1016/j.biotechadv.2011.06.019.
36. Gross, B.C.; Erkal, J.L.; Lockwood, S.Y.; Chen, C.; Spence, D.M. Evaluation of 3D Printing and Its Potential Impact on Biotechnology and the Chemical Sciences. *Analytical Chemistry* **2014**, *86*, 3240–3253, doi:10.1021/ac403397r.
37. Plesec, V.; Humar, J.; Dobnik-Dubrovski, P.; Harih, G. Numerical Analysis of a Transtibial Prosthesis Socket Using 3D-Printed Bio-Based PLA. *Materials* **2023**, *16*, doi:10.3390/ma16051985.
38. Milenkovic, S.; Slavkovic, V.; Fragassa, C.; Grujovic, N.; Palic, N.; Zivic, F. Effect of the Raster Orientation on Strength of the Continuous Fiber Reinforced PVDF/PLA Composites, Fabricated by Hand-Layup and Fused Deposition Modeling. *Composite Structures* **2021**, *270*, 114063, doi:https://doi.org/10.1016/j.compstruct.2021.114063.
39. Senatov, F.S.; Niaza, K.V.; Zadorozhnyy, M.Y.; Maksimkin, A.V.; Kaloshkin, S.D.; Estrin, Y.Z. Mechanical Properties and Shape Memory Effect of 3D-Printed PLA-Based Porous Scaffolds. *Journal of the Mechanical Behavior of Biomedical Materials* **2016**, *57*, 139–148, doi:10.1016/j.jmbbm.2015.11.036.
40. Slavkovic, V.; Palic, N.; Milenkovic, S.; Zivic, F.; Grujovic, N. Thermo-Mechanical Characterization of 4D-Printed Biodegradable Shape-Memory Scaffolds Using Four-Axis 3D-Printing System. *Materials* **2023**, *16*, doi:10.3390/ma16145186.
41. Bodaghi, M.; Namvar, N.; Yousefi, A.; Teymouri, H.; Demoly, F.; Zolfagharian, A. Metamaterial Boat Fenders with Supreme Shape Recovery and Energy Absorption/Dissipation via FFF 4D Printing. *Smart Materials and Structures* **2023**, *32*, 095028, doi:10.1088/1361-665X/acedde.
42. Pham, D.B.; Huang, S.-C. A Novel Bio-Inspired Hierarchical Tetrachiral Structure That Enhances Energy Absorption Capacity. *Journal of Mechanical Science and Technology* **2023**, *37*, 3229–3237, doi:10.1007/s12206-023-2202-y.
43. Choudhry, N.K.; Panda, B.; Dixit, U.S. Energy Absorption Characteristics of Fused Deposition Modeling 3D Printed Auxetic Re-Entrant Structures: A Review. *Journal of Materials Engineering and Performance* **2023**, *32*, 8981–8999, doi:10.1007/s11665-023-08243-3.
44. Gisario, A.; Desole, M.P.; Mehrpouya, M.; Barletta, M. Energy Absorbing 4D Printed Meta-Sandwich Structures: Load Cycles and Shape Recovery. *The International Journal of Advanced Manufacturing Technology* **2023**, *127*, 1779–1795, doi:10.1007/s00170-023-11638-0.
45. Novak, N.; Plesec, V.; Harih, G.; Cupar, A.; Kaljun, J.; Vesenjak, M. Development, Fabrication and Mechanical Characterisation of Auxetic Bicycle Handlebar Grip. *Scientific Reports* **2023**, *13*, 8158, doi:10.1038/s41598-023-35418-8.
46. Zhao, W.; Yue, C.; Liu, L.; Leng, J.; Liu, Y. Mechanical Behavior Analyses of 4D Printed Metamaterials Structures with Excellent Energy Absorption Ability. *Composite Structures* **2023**, *304*, 116360, doi:https://doi.org/10.1016/j.compstruct.2022.116360.

47. Bodaghi, M.; Serjouei, A.; Zolfagharian, A.; Fotouhi, M.; Rahman, H.; Durand, D. Reversible Energy Absorbing Meta-Sandwiches by FDM 4D Printing. *International Journal of Mechanical Sciences* **2020**, *173*, 105451, doi:https://doi.org/10.1016/j.ijmecsci.2020.105451.
48. Rahmatabadi, D.; Ghasemi, I.; Baniassadi, M.; Abrinia, K.; Baghani, M. 4D Printing of PLA-TPU Blends: Effect of PLA Concentration, Loading Mode, and Programming Temperature on the Shape Memory Effect. *Journal of Materials Science* **2023**, *58*, 7227–7243, doi:10.1007/s10853-023-08460-0.
49. Morvayova, A.; Contuzzi, N.; Fabbiano, L.; Casalino, G. Multi-Attribute Decision Making: Parametric Optimization and Modeling of the FDM Manufacturing Process Using PLA/Wood Biocomposites. *Materials* **2024**, *17*, doi:10.3390/ma17040924.
50. Song, Y.; Li, Y.; Song, W.; Yee, K.; Lee, K.-Y.; Tagarielli, V.L. Measurements of the Mechanical Response of Unidirectional 3D-Printed PLA. *Materials and Design* **2017**, *123*, 154–164, doi:https://doi.org/10.1016/j.matdes.2017.03.051.
51. Luo, J.; Luo, Q.; Zhang, G.; Li, Q.; Sun, G. On Strain Rate and Temperature Dependent Mechanical Properties and Constitutive Models for Additively Manufactured Polylactic Acid (PLA) Materials. *Thin-Walled Structures* **2022**, *179*, 109624, doi:https://doi.org/10.1016/j.tws.2022.109624.
52. Pepelnjak, T.; Karimi, A.; Maček, A.; Mole, N. Altering the Elastic Properties of 3D Printed Poly-Lactic Acid (PLA) Parts by Compressive Cyclic Loading. *Materials* **2020**, *13*, doi:10.3390/ma13194456.
53. Chen, W.; Guo, C.; Zuo, X.; Zhao, J.; Peng, Y.; Wang, Y. Experimental and Numerical Investigation of 3D Printing PLA Origami Tubes under Quasi-Static Uniaxial Compression. *Polymers* **2022**, *14*, doi:10.3390/polym14194135.
54. Qin, D.; Sang, L.; Zhang, Z.; Lai, S.; Zhao, Y. Compression Performance and Deformation Behavior of 3D-Printed PLA-Based Lattice Structures. *Polymers* **2022**, *14*, doi:10.3390/polym14051062.
55. Liu, T.; Liu, L.; Zeng, C.; Liu, Y.; Leng, J. 4D Printed Anisotropic Structures with Tailored Mechanical Behaviors and Shape Memory Effects. *Composites Science and Technology* **2020**, *186*, 107935, doi:https://doi.org/10.1016/j.compscitech.2019.107935.
56. Mercado-Colmenero, J.M.; Rubio-Paramio, M.A.; la Rubia-Garcia, M.D.; Lozano-Arjona, D.; Martin-Doñate, C. A Numerical and Experimental Study of the Compression Uniaxial Properties of PLA Manufactured with FDM Technology Based on Product Specifications. *The International Journal of Advanced Manufacturing Technology* **2019**, *103*, 1893–1909, doi:10.1007/s00170-019-03626-0.
57. Peng, X.; Liu, G.; Li, J.; Wu, H.; Jia, W.; Jiang, S. Compression Property and Energy Absorption Capacity of 4D-Printed Deformable Honeycomb Structure. *Composite Structures* **2023**, *325*, 117591, doi:https://doi.org/10.1016/j.compstruct.2023.117591.
58. Cadete, M.S.; Gomes, T.E.P.; Gonçalves, I.; Neto, V. Influence of 3D-Printing Deposition Parameters on Crystallinity and Morphing Properties of PLA-Based Materials. *Progress in Additive Manufacturing* **2024**, doi:10.1007/s40964-024-00608-x.
59. Barletta, M.; Gisario, A.; Mehrpouya, M. 4D Printing of Shape Memory Polylactic Acid (PLA) Components: Investigating the Role of the Operational Parameters in Fused Deposition Modelling (FDM). *Journal of Manufacturing Processes* **2021**, *61*, 473–480, doi:https://doi.org/10.1016/j.jmapro.2020.11.036.
60. Brischetto, S.; Torre, R. Tensile and Compressive Behavior in the Experimental Tests for PLA Specimens Produced via Fused Deposition Modelling Technique. *Journal of Composites Science* **2020**, *4*, doi:10.3390/jcs4030140.
61. Cláudio, R.A.; Dupont, J.; Baptista, R.; Leite, M.; Reis, L. Behaviour Evaluation of 3D Printed Polylactic Acid under Compression. *Journal of Materials Research and Technology* **2022**, *21*, 4052–4066, doi:https://doi.org/10.1016/j.jmrt.2022.10.042.
62. JI, Q.; Wei, J.; YI, J.; Zhang, L.; Ma, J.; Wang, Z. Study on the Static and Dynamic Mechanical Properties and Constitutive Models of 3D Printed PLA and PLA-Cu Materials. *Materials Today Communications* **2024**, *39*, 108690, doi:https://doi.org/10.1016/j.mtcomm.2024.108690.
63. Hosseini, S.A.; Torabizadeh, M.; Eisazadeh, H. Experimental Study of the Effect of Strain Rate on the Mechanical Behavior of Assorted Thermoplastic Polymers. *Journal of Materials Engineering and Performance* **2023**, doi:10.1007/s11665-023-08452-w.
64. Xu, P.; Lan, X.; Zeng, C.; Zhang, X.; Zhao, H.; Leng, J.; Liu, Y. Compression Behavior of 4D Printed Metamaterials with Various Poisson's Ratios. *International Journal of Mechanical Sciences* **2024**, *264*, 108819, doi:https://doi.org/10.1016/j.ijmecsci.2023.108819.
65. Rajkumar, A.R.; Shanmugam, K. Additive Manufacturing-Enabled Shape Transformations via FFF 4D Printing. *Journal of Materials Research* **2018**, *33*, 4362–4376, doi:10.1557/jmr.2018.397.
66. Balasubramanian, M.; Saravanan, R.; Shanmugam, V. Impact of Strain Rate on Mechanical Properties of Polylatic Acid Fabricated by Fusion Deposition Modeling. *Polymers for Advanced Technologies* **2024**, *35*, e6335, doi:https://doi.org/10.1002/pat.6335.
67. Bergström, J.S.; Boyce, M.C. Constitutive Modeling of the Large Strain Time-Dependent Behavior of Elastomers. *Journal of the Mechanics and Physics of Solids* **1998**, *46*, 931–954, doi:https://doi.org/10.1016/S0022-5096(97)00075-6.

68. Qi, H.J.; Boyce, M.C. Constitutive Model for Stretch-Induced Softening of the Stress–Stretch Behavior of Elastomeric Materials. *Journal of the Mechanics and Physics of Solids* **2004**, *52*, 2187–2205, doi:https://doi.org/10.1016/j.jmps.2004.04.008.
69. Qi, H.J.; Nguyen, T.D.; Castro, F.; Yakacki, C.M.; Shandas, R. Finite Deformation Thermo-Mechanical Behavior of Thermally Induced Shape Memory Polymers. *Journal of the Mechanics and Physics of Solids* **2008**, *56*, 1730–1751, doi:10.1016/j.jmps.2007.12.002.
70. Bodaghi, M.; Damanpack, A.R.; Liao, W.H. Triple Shape Memory Polymers by 4D Printing. *Smart Materials and Structures* **2018**, *27*, 065010, doi:10.1088/1361-665X/aabc2a.
71. Garg, M.; Mulliken, A.D.; Boyce, M.C. Temperature Rise in Polymeric Materials During High Rate Deformation. *Journal of Applied Mechanics* **2008**, *75*, 011009, doi:10.1115/1.2745388.
72. Ames, N.M.; Srivastava, V.; Chester, S.A.; Anand, L. A Thermo-Mechanically Coupled Theory for Large Deformations of Amorphous Polymers. Part II: Applications. *International Journal of Plasticity* **2009**, *25*, 1495–1539, doi:https://doi.org/10.1016/j.ijplas.2008.11.005.
73. Okereke, M.I.; Buckley, C.P.; Siviour, C.R. Compression of Polypropylene across a Wide Range of Strain Rates. *Mechanics of Time-Dependent Materials* **2012**, *16*, 361–379, doi:10.1007/s11043-012-9167-z.
74. Hao, P.; Spronk, S.W.F.; Paepegem, W.V.; Gilabert, F.A. Hydraulic-Based Testing and Material Modelling to Investigate Uniaxial Compression of Thermoset and Thermoplastic Polymers in Quasistatic-to-Dynamic Regime. *Materials & Design* **2022**, *224*, 111367, doi:https://doi.org/10.1016/j.matdes.2022.111367.
75. Bodaghi, M.; Damanpack, A.R.; Liao, W.H. Self-Expanding/Shrinking Structures by 4D Printing. *Smart Materials and Structures* **2016**, *25*, 105034, doi:10.1088/0964-1726/25/10/105034.
76. Van Manen, T.; Janbaz, S.; Jansen, K.M.B.; Zadpoor, A.A. 4D Printing of Reconfigurable Metamaterials and Devices. *Commun Mater* **2021**, *2*, 56, doi:10.1038/s43246-021-00165-8.
77. Staszczak, M.; Nabavian Kalat, M.; Golasiński, K.M.; Urbański, L.; Takeda, K.; Matsui, R.; Pieczyska, E.A. Characterization of Polyurethane Shape Memory Polymer and Determination of Shape Fixity and Shape Recovery in Subsequent Thermomechanical Cycles. *Polymers* **2022**, *14*, 4775, doi:10.3390/polym14214775.
78. Miehe, C.; Göktepe, S.; Méndez Diez, J. Finite Viscoplasticity of Amorphous Glassy Polymers in the Logarithmic Strain Space. *International Journal of Solids and Structures* **2009**, *46*, 181–202, doi:10.1016/j.ijsolstr.2008.08.029.
79. Boyce, M.C.; Arruda, E.M.; Jayachandran, R. The Large Strain Compression, Tension, and Simple Shear of Polycarbonate. *Polymer Engineering and Science* **1994**, *34*, 716–725.
80. Wiersma, J.; Sain, T. A Coupled Viscoplastic-Damage Constitutive Model for Semicrystalline Polymers. *Mechanics of Materials* **2023**, *176*, 104527, doi:https://doi.org/10.1016/j.mechmat.2022.104527.